water

MDPI

Article

# Channel Planform Dynamics Monitoring and Channel Stability Assessment in Two Sediment-Rich Rivers in Taiwan

**Cheng-Wei Kuo [1,*], Chi-Farn Chen [2], Su-Chin Chen [1], Tun-Chi Yang [3] and Chun-Wei Chen [2]**

[1] Department of Soil and Water Conservation, National Chung Hsing University, 145 Xingda Rd., South Dist., Taichung, 402, Taiwan; scchen@nchu.edu.tw (S.-C.C.)
[2] Center for Space and Remote Sensing Research, National Central University, 300 Jhongda Rd., Jhongli Dist., Taoyuan, 32001, Taiwan; cfchen@csrsr.ncu.edu.tw (C.-F.C.); wayne@csrsr.ncu.edu.tw (C.-W.C.)
[3] Water Administration Division, Water Resources Agency, Ministry of Economic Affairs, 501,Sec. 2, Liming Rd., Nantun Dist., Taichung 408, Taiwan; a660250@wra.gov.tw (T.-C.Y.)
* Correspondence: cwkuo7215@gmail.com; Tel.: +886-4-22840238; Fax: +886-22853967

Academic Editor: Peggy A. Johnson
Received: 30 November 2016; Accepted: 25 January 2017; Published: 30 January 2017

**Abstract:** Recurrent flood events induced by typhoons are powerful agents to modify channel morphology in Taiwan's rivers. Frequent channel migrations reflect highly sensitive valley floors and increase the risk to infrastructure and residents along rivers. Therefore, monitoring channel planforms is essential for analyzing channel stability as well as improving river management. This study analyzed annual channel changes along two sediment-rich rivers, the Zhuoshui River and the Gaoping River, from 2008 to 2015 based on satellite images of FORMOSAT-2. Channel areas were digitized from mid-catchment to river mouth (~90 km). Channel stability for reaches was assessed through analyzing the changes of river indices including braid index, active channel width, and channel activity. In general, the valley width plays a key role in braided degree, active channel width, and channel activity. These indices increase as the valley width expands whereas the braid index decreases slightly close to the river mouth due to the change of river types. This downstream pattern in the Zhuoshui River was interrupted by hydraulic construction which resulted in limited changes downstream from the weir, due to the lack of water and sediment supply. A 200-year flood, Typhoon Morakot in 2009, induced significant changes in the two rivers. The highly active landscape in Taiwan results in very sensitive channels compared to other regions. An integrated Sensitivity Index was proposed for identifying unstable reaches, which could be a useful reference for river authorities when making priorities in river regulation strategy. This study shows that satellite image monitoring coupled with river indices analysis could be an effective tool to evaluate spatial and temporal changes in channel stability in highly dynamic river systems.

**Keywords**: channel stability; sensitivity index; satellite images; typhoons; braid index

## 1. Introduction

Patterns of river channel planform dynamics reflect a variety of flow and sediment regimes which are controlled by climatic and geologic conditions [1]. Taiwan is located on the track of typhoons in the Western Pacific Ocean and experiences 3–4 typhoons per year on average. Recurrent flood events induced by typhoons are powerful agents to modify channel morphology in Taiwan's rivers. In addition, abundant sediment supply due to fragile geology and frequent landslides in Taiwan's landscapes provides materials along the river network for reforming channels and floodplains. Frequent channel migrations reflect highly sensitive valley floors and increase the risk to infrastructure and residents along rivers. Ideal river engineering is able to mitigate flood hazards,

and this must be based on a good understanding of river characteristics in terms of spatial and temporal variations. An assessment of channel variations is necessary by river authorities as well as by ecologists for better management of river ecosystems [2]. In this sight, fluvial geomorphology should be integral to the planning, implementation, and post-project appraisal stages of engineering projects [3].

Braided rivers, characterized by unstable channel courses and rapid changes, always interest fluvial geomorphologists. They have focused on topics such as confluence scour [4], sediment transport and morphological changes [5] in braided river systems. The types of braid index and the effect of water level have been also investigated [6]. Traditional channel change analysis relies on repeated field surveys which are time-consuming and have a limited spatial scale. In the past two decades, a great advance in remote sensing technology expands the scope of river studies both in spatial and temporal scales. Techniques of remote sensing have been widely applied to river change studies. Based on aerial photograph analysis, researchers can join traditional maps to analyze long-term island changes and channel expansion/narrowing [7], or combine field surveys to evaluate the impact of changing sediment flux on braided river evolution [8] and also to observe sediment pulses after bend cutoffs in wandering rivers [9]. Moreover, remote sensing from satellites can capture recurrent images and have multi-spectral sensors, becoming a powerful tool to monitor changes on the earth's surface over a large area. Satellite images can couple with GIS tools to analyze changes in braid index and channel width [10] or apply supervised/unsupervised classification to monitor channel numbers and bar changes [11,12].

For practical proposes in river management, the information from these analyses could be simplified into indices of channel stability, as indicators to assess the overall situation within a river basin. Nelson et al. [13] analyzed changes in braid index, channel width, channel activity, and net channel change based on a series of aerial photographs of the Snake River in Grand Teton National Park, USA. These calculations are useful to evaluate the channel change and stability and could be developed further. Large-scale channel stability analysis should consider the spatial difference along study rivers. The impact of floods on channel morphology is highly variable. Spatial variations of channel characteristics, such as valley confinement, channel configuration, and bed materials texture influence channel responses to flood events along a river [14]. For reaches with abundant sediment input, an extreme event could induce significant deposition on the valley floor, causing valley expansion and channel shifting. However, channel incision and narrowing may occur as long as sediment input decreases, thus a braid river may transform into a wandering river [15–17].

This study used high spatial resolution (2 m) satellite images from FORMOSAT-2 to analyze annual channel planform changes along the Zhuoshui River and Gaoping River in Taiwan from 2008 to 2015. Three river indices, including braid index, active channel width, and channel activity, were involved in the numerical analysis to evaluate the channel stability and the impact of hydrological events. An integrated index named Sensitivity Index was proposed for identifying unstable reaches. These results could provide implications for river regulation and management in highly dynamic river systems.

## 2. Study Area

The Zhuoshui River originates from the Hehuan Mountain area with an elevation of ~3220 m a.s.l. to the Taiwan Strait (Figure 1). The drainage area is ~3157 $km^2$ and the length of the mainstream is ~186.6 km, which makes it the longest river in Taiwan. The geology of the mountain area is composed of fragile slate, shale, and sandstone. These materials are easily eroded and transported by river channels. The name "Zhuoshui" means turbid water, which implies stream water with a high sediment concentration. The sediment yield is 13,000 $t \cdot km^{-2} \cdot year^{-1}$, which is higher than the average for rivers in Taiwan (9500 $t \cdot km^{-2} \cdot year^{-1}$). Sediment yield in the Zhuoshui River is 86-fold greater than the global yield (150 $t \cdot km^{-2} \cdot year^{-1}$) [18]. The difference of spatial and temporal rainfall distribution is quite evident. The annual rainfall is ~2500 mm, but decreases from the mountain area (~4000mm) to the lowland plain (~1500 mm). More than 75% of rainfall occurs during wet seasons (from May to October), especially during typhoon events. Abundant sediment supply couples with frequent flood

events, resulting in sensitive channels. The downstream reach in the plain area had experienced severe flood hazards and the channel migrated greatly several times before the twentieth century. Long-term channel migrations created the largest alluvial fan in Taiwan (~1800 km$^2$) which provided a proper environment for agriculture. To protect residents and infrastructure along the downstream area, embankments have been built since 1911 to constrain the river course. In addition, the Jiji Weir was constructed in 2001 for providing domestic, industry and agricultural water use for the downstream plain. This structure inevitably altered the water and sediment flux downstream.

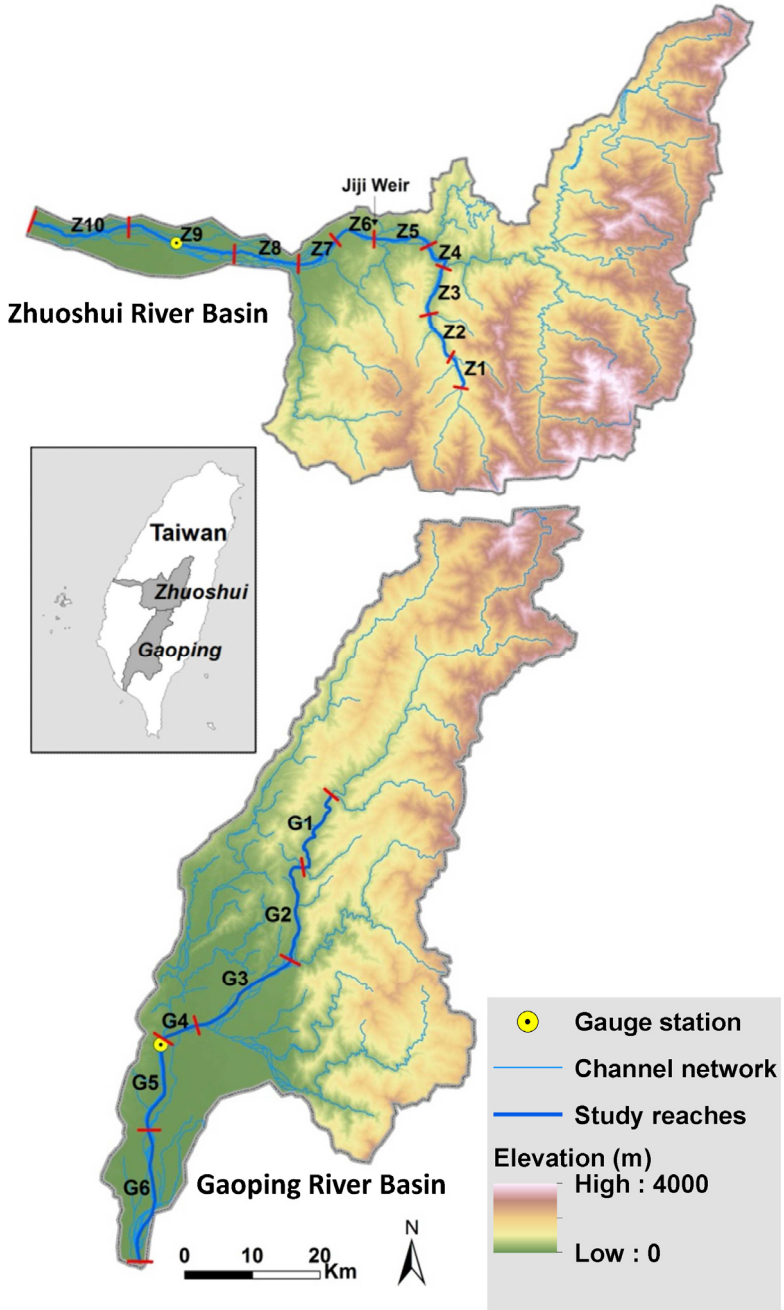


**Figure 1.** The location and terrain of the Zhuoshui and Gaoping River Basins. Study reaches are tagged (Z1~Z10 and G1~G6) and divided by red bars.

The Gaoping River generates from the Mt. Jade East Peak (3869 m) and has the largest drainage area (3527 km$^2$) and the second longest mainstream length (171 km) of Taiwan's rivers (Figure 1). The mountain area is underlain by slate, shale, sandstone and mudstone. The annual average rainfall is 3000 mm and the difference of spatial and temporal rainfall distribution is also quite evident in the

Gaoping River Basin. Rainfall in the mountain area (~4000 mm) is much higher than in the lowland plain (~2000 mm). The seasonal rainfall distribution is highly concentrated from May to September (~90%). The sediment yield is 6500 t $km^{-2}$ $year^{-1}$ which is lower than the Zhuoshui River but still very high [18]. The severest sediment disaster occurred on 9 August 2009. Typhoon Morakot dumped more than 2000 mm of rainfall, over 70% of the average annual rainfall, on southwestern Taiwan. The heavy rainfall triggered 12,697 landslides, including four giant landslides, with a total area of 183.1 $km^2$ [19]. To protect the villages, agricultural and industrial areas from flood hazards, an embankment more than 20 km long was built along the most downstream reach. In addition, the Gaoping River Weir was constructed in the downstream area in 1999 for providing water use for the Kaohsiung area.

This study focused on the channel changes from the middle to downstream area because the upstream channels are confined by steep valleys, thus no notable changes are observed there. The total lengths of the study reaches are 93.6 km for the Zhuoshui River and 88.2 km for the Gaoping River. For the upper study reaches in the hilly area of the Zhuoshui River, one tributary named Chenyoulan River was chosen for analysis rather than the mainstream because this tributary has a wider valley floor and more active channels, bars, and floodplains than the mainstream. The upper section of the mainstream of the Gaoping River is called the Laonong River, and was included in the channel change analysis.

Before evaluating the channel stability, the study area needed to be divided into reaches with similar channel types. Here we used three criteria for dividing the channels. They are: confluence with tributary, evident changes of valley width, and hydraulic construction. Water and sediment influx from tributaries could modify the configuration of channels and bars along the river mainstream. Sudden change of valley width could decrease the flow velocity, thus prompting sediment deposition. Hydraulic constructions could disrupt longitudinal conveyance of sediment, causing the discontinuity of river course and sediment transport. Following these criteria, the study reaches were separated into ten divisions in the Zhuoshui River and six in the Gaoping River. The spatial patterns of these divisions are shown in Figure 1. The boundaries between reaches and environmental attributes are listed in Table 1. The last column is "valley setting," which indicates the degree of river channels abut valley margins. A confined river is a channel that abuts a bedrock valley margin along more than 90% of its length. By contrast, a laterally-unconfined river has less than 10% of length abutting a valley margin. For a partly confined river, the percentage is between 10% and 90% [20]. Valley setting implies the potential for channel migration.

## 3. Methods

### *3.1. Satellite Image Collection and Channel Digitizing*

The FORMOSAT-2 is the first remote sensing satellite developed by the National Space Organization (NSPO), Taiwan. It was launched in 2004 into the Sun-synchronous orbit located 891 km above the ground. The resolution is 2 m for panchromatic images and 8 m for color images. This study used color images of 2 m resolution after processing image fusion. In order to monitor annual channel change, one image per year needs to be extracted for the channel mapping and analysis. However, the scan swath of FORMOSAT-2 is 24 km and the scan direction is north-south, which is perpendicular to the flow directions of the rivers in the Western Taiwan. Thus, the images need to be obtained from different dates to cover the whole study reaches. Monitoring the whole study reaches needs four stripes of images of the Zhuoshui River and two stripes of the Gaoping River. For each year, images for channel digitizing were chosen from the wet seasons (May to October) in order to observe more active channels at high water levels. After mosaicking images on different but near dates, the channel area (water body) along the Zhuoshui and Gaoping River were digitized as polygon features by using ArcGIS 10.2 (ESRI, Redlands, CA, USA) from 2008 to 2015.

**Table 1.** Boundaries and attributes of study reaches.

| Basin | Reach ID | Upstream Boundary | Length (km) | Elevation (m) | Valley Slope | Average Valley Width (m) | Valley Setting |
|---|---|---|---|---|---|---|---|
| Zhuoshui River | Z1 | Confluence of Alibudong Stream | 5.6 | 586–708 | 0.0219 | 303 | Partly-confined |
| | Z2 | Confluence of Shibachong Stream | 8.0 | 440–586 | 0.0183 | 376 | Partly-confined |
| | Z3 | Confluence of Junkeng Stream | 8.0 | 308–440 | 0.0165 | 481 | Partly-confined |
| | Z4 | Confluence of Chenyoulan | 5.3 | 266–308 | 0.0079 | 450 | Partly-confined |
| | Z5 | Yufeng Bridge (Confluence of Shuili Stream) | 9.2 | 196–266 | 0.0076 | 730 | Laterally-unconfined |
| | Z6 | Jiji Weir | 6.7 | 152–196 | 0.0065 | 364 | Confined |
| | Z7 | Mingzhu Bridge | 7.4 | 99–152 | 0.0072 | 1000 | Laterally-unconfined |
| | Z8 | Confluence of Qingshui Stream | 10.3 | 52–99 | 0.0046 | 1514 | Laterally-unconfined |
| | Z9 | Dazhuang Village | 17.2 | 16–52 | 0.0021 | 1083 | Laterally-unconfined |
| | Z10 | Ziqiang Bridge | 16.0 | 0–16 | 0.0010 | 1448 | Laterally-unconfined |
| Gaoping River | G1 | Baolai Bridge (confluence of Baolai Stream) | 14.7 | 251–369 | 0.0081 | 287 | Partly-confined |
| | G2 | Dongxi Bridge (confluence of Bangfu stream) | 15.9 | 141–251 | 0.0069 | 539 | Partly-confined |
| | G3 | Dajin Bridge (confluence of Zhuokou stream) | 17.6 | 31–141 | 0.0063 | 1722 | Laterally-unconfined |
| | G4 | Ligang Bridge (confluence of Ailiao stream) | 6.2 | 24–31 | 0.0012 | 1753 | Laterally-unconfined |
| | G5 | Liling Bridge (confluence of Qishan stream) | 13.8 | 12–24 | 0.0009 | 1566 | Laterally-unconfined |
| | G6 | Gaoping River Weir | 20.0 | 0–12 | 0.0006 | 2047 | Laterally-unconfined |

For putting the channel changes in the context of hydrological events, the daily discharge data were collected from two long-term gauge stations with continuous records. Station Xizhou Bridge on the Zhuoshui River has operated since 2001 with a drainage area of 2894 km². Station Liling Bridge on the Gaoping River has operated since 1994 with a drainage area of 2975 km². The hydrographs of daily discharge during the study period are shown in Figure 2. The locations of the stations are marked on Figure 1. The captured dates of images are marked by crosses on Figure 2. The corresponding values on the left y-axis show the water level on the dates of images. The differences of the water level are all less than 0.5 m within each year. The range of the water level between different years is 20.14~21.26 m in Station Xizhou Bridge and 22.34~24.60 in Station Liling Bridge. Slightly changes of the water level could influence the area of exposed channel bars, but have a low impact on calculating numbers and lengths of channels.

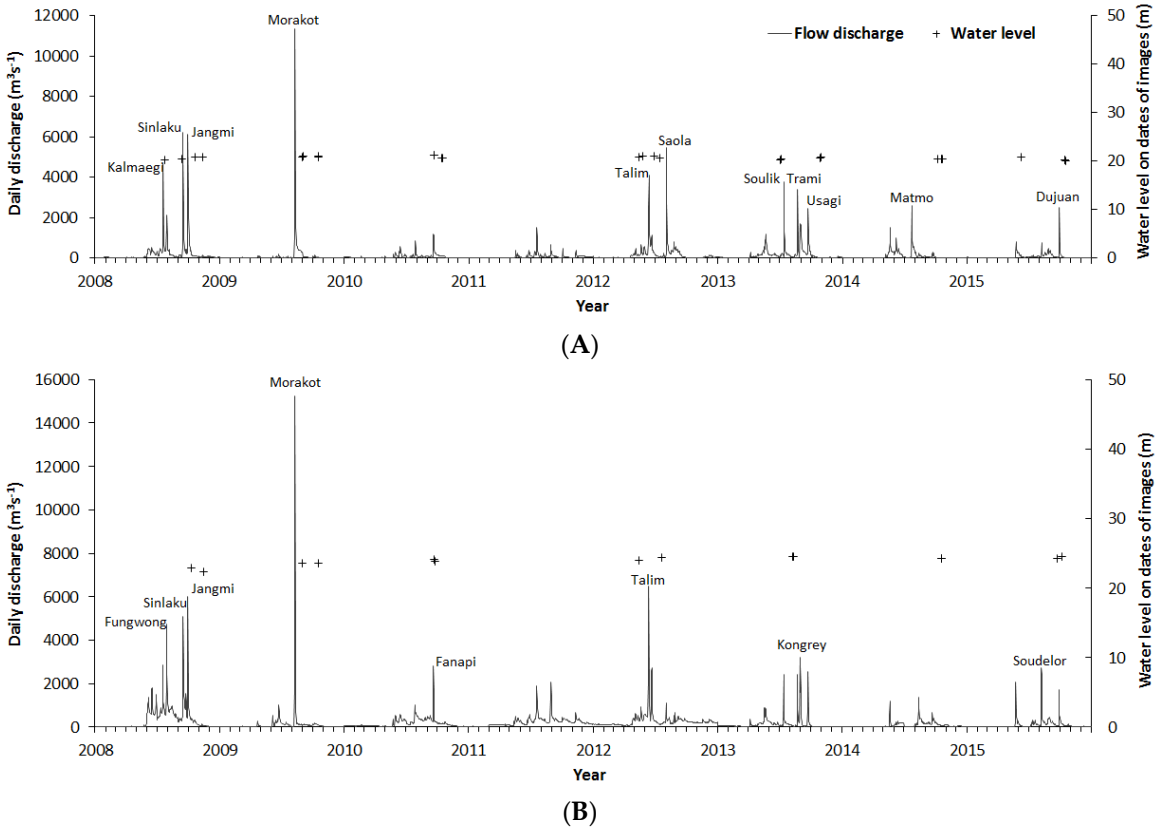


**Figure 2.** The hydrographs of daily discharge at flow gauge station Xizhou Bridge on the Zhuoshui River (**A**); and Liling Bridge on the Gaoping River (**B**). The locations of stations are marked on Figure 1. The names of typhoons are tagged on flow peaks. Crosses indicate water levels on dates of satellite images. The exact dates in 2011 are missing.

### *3.2. Channel Stability Analysis*

Channel stability is evaluated through the calculation and analysis of channel planform indices including braid index, active channel width, and annual channel activity [13]. Before calculating these indices, it is necessary to obtain active channel area (polygon feature) and channel length (line feature). In this study, active channels refer to wetted channels; dry channels on lateral bars and floodplains are excluded. The central line of a channel area could be extracted in ArcGIS (ESRI). The calculation methods for indices are explained as follows. Braid index (*BI*) is calculated by dividing the total channel length, including all active secondary channels ($\Sigma L_S$), by the main channel length ($\Sigma L_M$) based on the centerline of the channels [21,22] (see Figure 3A). A greater braid index implies an unstable river condition. Active channel width (*CW*) is calculated by dividing the channel area (*Ac*) by the centerline length of the main channel ($\Sigma L_M$). Annual channel activity (*CA*) is the combined area

of erosion and deposition of the active channel per year per unit longitudinal distance. Channel activity is an indicator of channel stability and the rate of channel migration. Erosion and deposition were determined by overlaying active channel positions within the GIS and identifying changes from floodplain to channel (erosion) or from channel to floodplain (deposition) among the image series (see Figure 3B).

In order to compare spatial variations of channel stability, we averaged values of different years reach by reach, then plotted downstream patterns of channel planform indices. On the other hand, we averaged values of different reaches year by year to examine the annual changes in view of the impacts of hydrological events. Finally, we calculated the coefficient of variance (CV = Standard deviation/Mean) of these three indices for each reach, then added them up to get the Sensitivity Index ($SI = CV_{BI} + CV_{CW} + CV_{CA}$). This index was used to assess an overall channel stability.

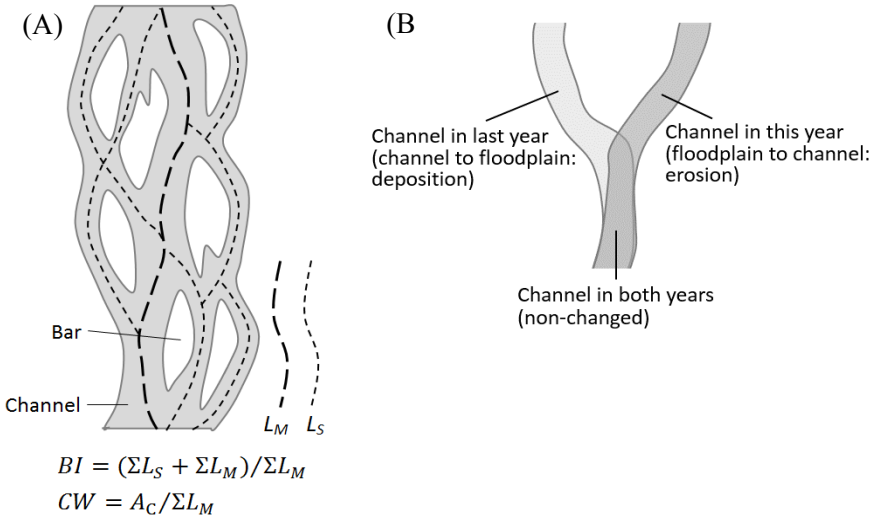


**Figure 3.** (**A**) Illustration for calculating braid index (*BI*) and active channel width (*CW*); (**B**) Illustration for categories of channel changes (erosion, deposition and non-changed). Notes for terms: $L_S$: the length of the secondary channels; $L_M$: the length of the main channel; *Ac:* the channel area.

## 4. Results

### *4.1. Downstream Patterns of Channel Planform Indices*

The results of calculating channel planform indices are listed by reach and by year in Table 2. The levels of values are shown by grayscale background for comparing the spatial and temporal variance. Firstly, average values during the study period for each reach were calculated to show the spatial patterns. Downstream patterns of braid index, active channel width, and channel activity in the Zhuoshui and Gaoping Rivers are shown in Figure 4. This figure was composed of the average value (black lines) and ±1 standard deviation (gray lines). The statistics of the three indices by reaches are listed in Table 3.

In terms of the downstream patterns in the Zhuoshui River, the braid index (Figure 4A) in the Chenyoulan River (Z1–Z4) increases gradually from 1.6 to 2.1. After entering the mainstream of the Zhuoshui River, the value increases to 2.7 (Z5) but drops suddenly to 1.4 (Z6). Obviously, this discontinuity of spatial changes is caused by the Jiji Weir. The braid index reaches the highest value of 3.3 when the valley expands greatly in Z7 and then decreases gradually to 2.8 close to the river mouth (Z10). Overall, the active channel width (Figure 4B) expands gradually from upstream to downstream but with a sudden drop in Z6. It is less than 100 m in the Chenyoulan River (Z1–Z4), then increases to more than 100 m after entering the mainstream. The active channel width reaches approximately 200 m close to the river mouth. The downstream pattern of channel activity (Figure 4C) has a similar trend with active channel width.

In terms of the downstream patterns in the Gaoping River, the braid index (Figure 4D) first increases then decreases to the end. The peak value of 2.9 occurs at G3, a reach transferring from the hilly area to the lowland plain. The change of active channel width (Figure 4E) shows a steady increasing trend from upstream to downstream. It is less than 100 m in the reaches with confined valleys (G1–G2) and larger than 200 m in reach G3 with an unconfined valley. After joining the main tributary, Ailiao River, the channel width expands to 300 m (G4) then continues to increase to 350 m (G6) close to the river mouth. Finally, the change of channel activity (Figure 4F) shows a trend with first an increase, then a decrease after reach G4.

**Table 2.** Channel planform indices are listed by reaches and years and shown in grayscale. The higher values are shown by the darker background.

| **(A) Braid index** | | | | | **Year** | | | |
|---|---|---|---|---|---|---|---|---|
| **Reach** | **2008** | **2009** | **2010** | **2011** | **2012** | **2013** | **2014** | **2015** |
| Z1 | 1.73 | 1.20 | 1.11 | 1.37 | 1.19 | 1.63 | 1.22 | 2.23 |
| Z2 | 1.91 | 1.27 | 1.14 | 1.43 | 1.56 | 2.83 | 1.68 | 1.89 |
| Z3 | 1.63 | 1.82 | 1.63 | 2.10 | 1.07 | 2.60 | 2.06 | 1.96 |
| Z4 | 2.36 | 2.28 | 1.20 | 1.44 | 1.61 | 3.86 | 1.90 | 1.85 |
| Z5 | 2.79 | 3.00 | 1.75 | 1.78 | 1.97 | 3.36 | 3.82 | 2.94 |
| Z6 | 1.54 | 1.55 | 1.34 | 1.24 | 1.15 | 2.02 | 1.31 | 1.07 |
| Z7 | 4.22 | 4.95 | 2.50 | 2.62 | 2.26 | 2.27 | 4.68 | 2.67 |
| Z8 | 2.91 | 4.60 | 3.62 | 2.44 | 2.31 | 2.71 | 3.06 | 1.98 |
| Z9 | 3.14 | 3.65 | 1.76 | 2.81 | 2.48 | 2.34 | 3.41 | 2.94 |
| Z10 | 2.45 | 2.53 | 1.96 | 3.16 | 2.16 | 3.31 | 3.73 | 3.12 |
| G1 | 1.81 | 1.47 | 1.17 | 1.47 | 1.30 | 1.65 | 1.42 | 1.55 |
| G2 | 2.07 | 2.16 | 1.48 | 2.33 | 1.53 | 1.38 | 1.86 | 1.77 |
| G3 | 3.59 | 3.83 | 2.04 | 2.34 | 3.56 | 2.05 | 2.85 | 2.53 |
| G4 | 2.97 | 1.69 | 2.05 | 2.93 | 2.85 | 2.07 | 2.50 | 2.54 |
| G5 | 2.31 | 1.73 | 1.75 | 2.62 | 2.75 | 2.49 | 3.10 | 2.07 |
| G6 | 2.07 | 2.23 | 1.67 | 2.33 | 3.30 | 2.66 | 2.80 | 1.93 |
| **(B) Active channel width (m)** | | | | | **Year** | | | |
| **Reach** | **2008** | **2009** | **2010** | **2011** | **2012** | **2013** | **2014** | **2015** |
| Z1 | 28 | 37 | 17 | 23 | 35 | 57 | 22 | 33 |
| Z2 | 29 | 62 | 19 | 28 | 45 | 107 | 36 | 32 |
| Z3 | 33 | 84 | 37 | 51 | 47 | 94 | 36 | 37 |
| Z4 | 91 | 165 | 54 | 52 | 115 | 172 | 61 | 57 |
| Z5 | 163 | 186 | 107 | 98 | 121 | 206 | 128 | 159 |
| Z6 | 115 | 118 | 42 | 55 | 52 | 73 | 37 | 31 |
| Z7 | 256 | 190 | 75 | 69 | 73 | 81 | 99 | 60 |
| Z8 | 300 | 295 | 123 | 92 | 96 | 69 | 77 | 70 |
| Z9 | 200 | 385 | 91 | 215 | 193 | 119 | 265 | 129 |
| Z10 | 227 | 290 | 166 | 262 | 338 | 207 | 153 | 154 |
| G1 | 83 | 159 | 36 | 58 | 46 | 53 | 33 | 50 |
| G2 | 117 | 232 | 74 | 100 | 70 | 57 | 48 | 65 |

| | | | | | | | | |
|---|---|---|---|---|---|---|---|---|
| G3 | 243 | 449 | 145 | 128 | 144 | 99 | 95 | 144 |
| G4 | 275 | 293 | 275 | 343 | 271 | 206 | 193 | 493 |
| G5 | 214 | 320 | 259 | 347 | 309 | 242 | 195 | 459 |
| G6 | 378 | 441 | 328 | 426 | 350 | 302 | 207 | 429 |

| **(C) Channel activity (ha/km/y)** | **Year** | | | | | | |
|---|---|---|---|---|---|---|---|
| **Reach** | **2008-2009** | **2009-2010** | **2010-2011** | **2011-2012** | **2012-2013** | **2013-2014** | **2014-2015** |
| Z1 | 5.1 | 5.6 | 3.2 | 4.7 | 5.9 | 4.2 | 3.2 |
| Z2 | 6.6 | 7.2 | 3.8 | 6.5 | 12.6 | 9.8 | 4.2 |
| Z3 | 9.8 | 10.3 | 6.1 | 6.3 | 10.6 | 8.8 | 4.9 |
| Z4 | 13.8 | 16.2 | 3.4 | 13.4 | 12.2 | 14.7 | 7.2 |
| Z5 | 19.0 | 17.2 | 10.1 | 12.9 | 23.3 | 19.6 | 15.3 |
| Z6 | 11.6 | 8.8 | 3.8 | 4.2 | 6.6 | 4.4 | 2.2 |
| Z7 | 35.1 | 17.4 | 4.3 | 8.3 | 13.4 | 13.8 | 9.6 |
| Z8 | 44.9 | 28.3 | 15.2 | 14.2 | 17.7 | 10.7 | 10.0 |
| Z9 | 44.2 | 38.3 | 23.2 | 28.0 | 27.3 | 25.0 | 22.5 |
| Z10 | 36.3 | 29.9 | 26.4 | 27.0 | 39.1 | 31.0 | 23.5 |
| G1 | 12.3 | 13.4 | 5.7 | 7.5 | 5.4 | 5.4 | 4.3 |
| G2 | 24.2 | 23.2 | 9.3 | 10.9 | 5.9 | 7.6 | 6.8 |
| G3 | 51.1 | 40.5 | 16.4 | 16.0 | 19.9 | 16.3 | 16.5 |
| G4 | 46.4 | 25.5 | 30.0 | 30.1 | 36.7 | 29.4 | 37.2 |
| G5 | 34.4 | 30.8 | 22.3 | 23.2 | 26.0 | 18.5 | 28.6 |
| G6 | 39.7 | 26.8 | 19.4 | 17.7 | 28.4 | 22.5 | 25.8 |

**Table 3.** Sensitivity index and statistics of braid index, active channel width, and channel activity for study reaches.

| **Reach** | **Braid Index** | | | **Active Channel Width (m)** | | | **Channel Activity (ha/km/year)** | | | **Sensitivity Index *** |
|---|---|---|---|---|---|---|---|---|---|---|
| | **Mean** | **S.D.** | **C.V.** | **Mean** | **S.D.** | **C.V.** | **Mean** | **S.D.** | **C.V.** | |
| Z1 | 1.46 | 0.36 | 24% | 32 | 12 | 37% | 4.57 | 1.00 | 22% | 83% L |
| Z2 | 1.72 | 0.49 | 29% | 45 | 26 | 59% | 7.25 | 2.87 | 40% | 127% M |
| Z3 | 1.86 | 0.42 | 22% | 53 | 22 | 42% | 8.11 | 2.15 | 27% | 91% L |
| Z4 | 2.06 | 0.77 | 37% | 96 | 47 | 49% | 11.54 | 4.21 | 37% | 123% M |
| Z5 | 2.68 | 0.72 | 27% | 146 | 36 | 25% | 16.76 | 4.09 | 24% | 76% L |
| Z6 | 1.40 | 0.28 | 20% | 65 | 32 | 49% | 5.97 | 3.02 | 51% | 120% M |
| Z7 | 3.27 | 1.07 | 33% | 113 | 67 | 59% | 14.55 | 9.27 | 64% | 155% H |
| Z8 | 2.95 | 0.78 | 26% | 140 | 92 | 66% | 20.17 | 11.55 | 57% | 149% H |
| Z9 | 2.81 | 0.57 | 20% | 200 | 88 | 44% | 29.79 | 7.63 | 26% | 90% L |
| Z10 | 2.80 | 0.58 | 21% | 225 | 64 | 28% | 30.45 | 5.16 | 17% | 66% L |
| G1 | 1.48 | 0.19 | 13% | 65 | 38 | 59% | 7.73 | 3.37 | 44% | 116% M |
| G2 | 1.82 | 0.32 | 18% | 95 | 56 | 58% | 12.55 | 7.20 | 57% | 133% H |
| G3 | 2.85 | 0.68 | 24% | 181 | 110 | 61% | 25.26 | 13.36 | 53% | 137% H |
| G4 | 2.45 | 0.44 | 18% | 294 | 87 | 30% | 33.62 | 6.50 | 19% | 67% L |
| G5 | 2.35 | 0.45 | 19% | 293 | 80 | 27% | 26.28 | 5.04 | 19% | 66% L |
| G6 | 2.37 | 0.49 | 21% | 358 | 74 | 21% | 25.76 | 6.74 | 26% | 68% L |

* Level of sensitivity: L = Low, M=Moderate, H = High. S.D: Standard deviation; C.V: Coefficient of variance

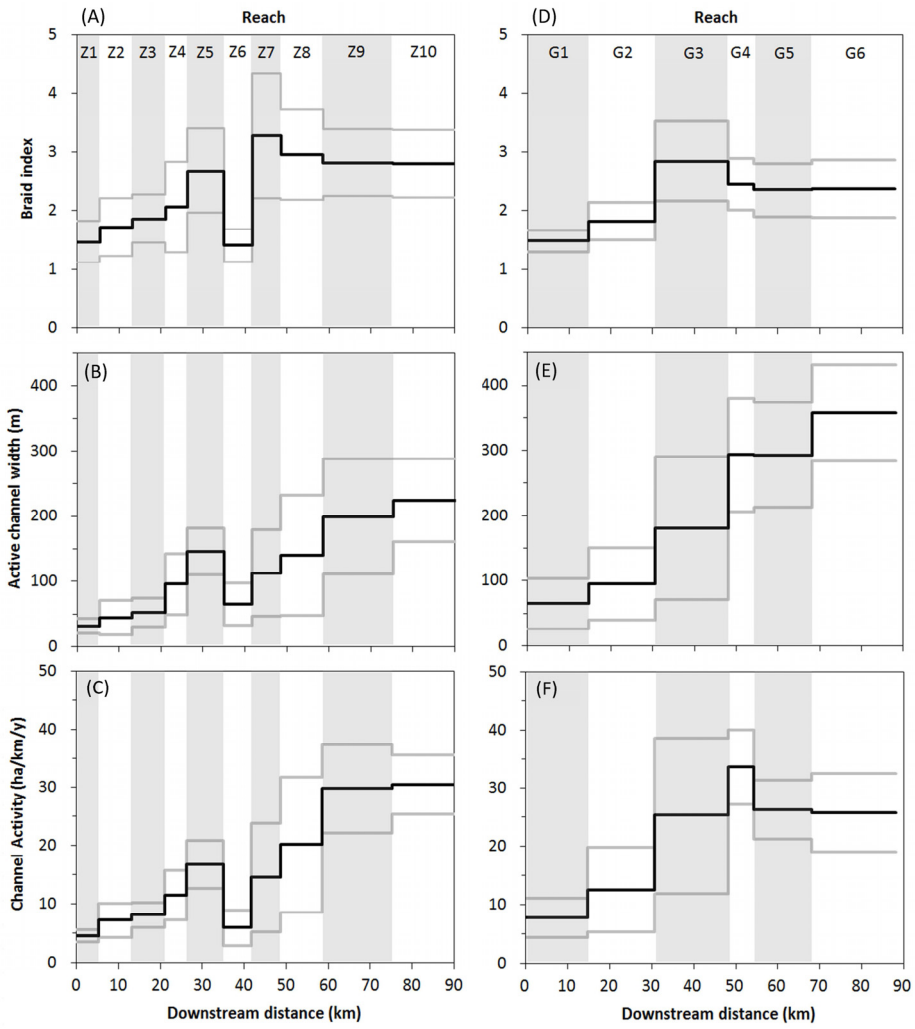


**Figure 4.** Downstream patterns of braid index, active channel width, and channel activity along the Zhuoshui River (**A**–**C**); and the Gaoping River (**D**–**F**) during 2008–2015. Black lines show the average values and grey lines show the ranges of ±1 standard deviation.

### *4.2. Annual Change of Erosion and Deposition*

This section explores the temporal changes in erosion (from floodplain to channel) and deposition (from channel to floodplain) areas in the study rivers. Here we added the areas of all of the study reaches from upstream to downstream for each period. Overall, the two graphs display similar patterns (Figure 5). The lines of annual erosion and deposition areas of these two rivers fluctuate in the same direction in almost every period except the last year. In terms of the non-changed areas, the values in the Zhuoshui River vary around 500 ha with no noticeable changes. The non-changed areas in the Gaoping River are over 1000 ha during the first half of the study period, but decrease greatly after 2013.

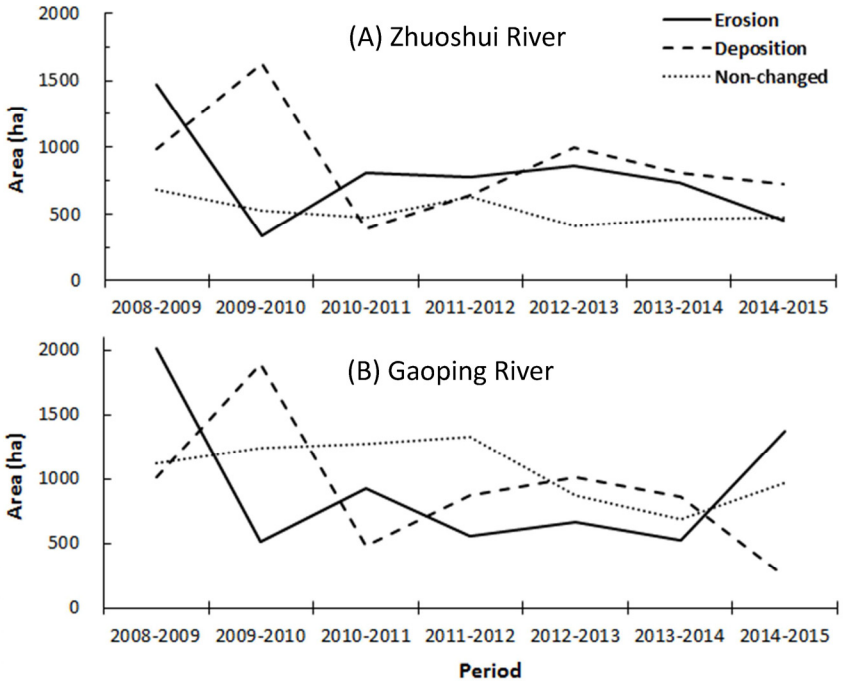


**Figure 5.** The annual changes for erosion, deposition and non-changed areas in the Zhuoshui River (**A**); and the Gaoping River (**B**).

*4.3 Assessment of Channel Stability*

For assessing and comparing channel stability between different reaches, the values of CV were used to derive the Sensitivity Index (SI). Basically, a higher CV represents a greater dispersion for yearly values, which implies an unstable condition within a reach. This study attempted to summarize the CV values of the three planform indices to get a Sensitivity Index (Table 3). A lower value of Sensitivity Index means that the reach is more stable. We categorized the SI into three levels: low (50%–100%), moderate (100%–130%) and high (>130%). This grading has advantages for simple evaluation and making a priority for regulation strategy in river management. To determine the boundaries for grading, the natural breaks between values were sought in order to reduce the variance within classes and increase the variance between classes. The spatial patterns of SI for the study reaches are shown in Figure 6.

For the Zhuoshui River (Figure 6A), reaches of low and moderate sensitivity alternate from Z1 to Z6. The most sensitive reaches appear at Z7, where the valley expands significantly, and Z8, where a large tributary named Qingshui Stream joins. The most downstream reaches (Z9 and Z10) are of low sensitivity. For the Gaoping River (Figure 6B), the upstream reach G1 is moderately sensitive, following the two highly sensitive reaches G2 and G3, and ending with three relative stable reaches, G4–G6.

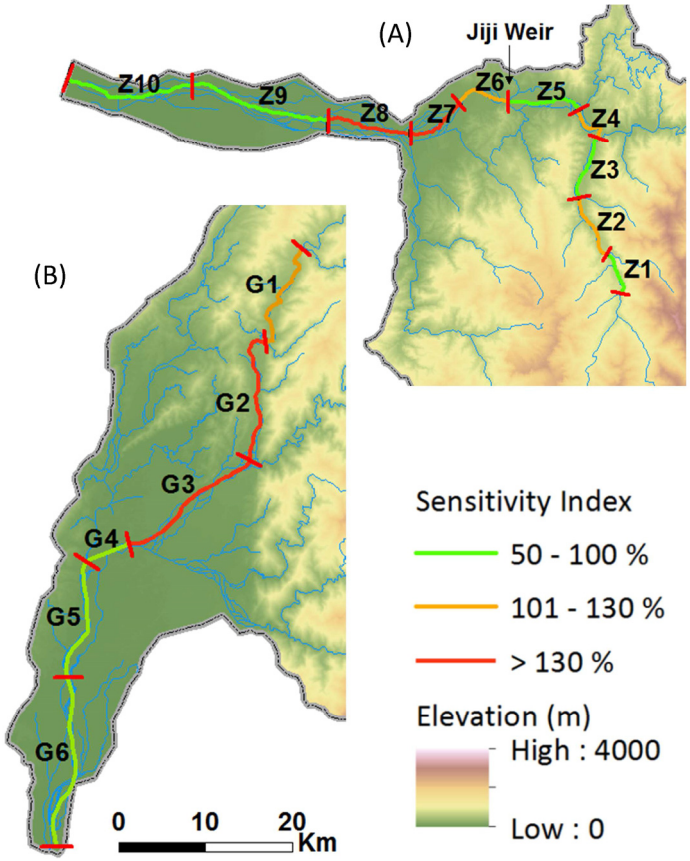


**Figure 6.** The downstream patterns of the Sensitivity Index along the Zhuoshui (**A**); and the Gaoping Rivers (**B**).

## 5. Discussion

### *5.1. The Influence of Valley Width and Hydraulic Construction upon Channel Planform Changes*

The downstream patterns of the channel planform indices show downstream increasing trends in general. This implies that the patterns should be related to the changes of valley width. We measured channel widths from the satellite images in 2015 by a sampling interval of 2 km from the upstream to downstream end of the study rivers. Each reach would get an average valley width. The relationships between valley widths and the three channel planform indices are described by x-y scatter plots (Figure 7). All the three indices have highly positive correlations with valley width (all of the correlation coefficients > 0.7). This finding indicates that valley width plays a key role in braided degree, active channel width, and channel activity. In terms of braid index, as long as the background environment has abundant sediment (mainly gravels and sands in this case), steep valley slope, and frequent flood events, the wider valley could provide more space for developing braided channels [23,24] and also main channel shifting [25]. The highest braid index occurs in Z7 in the Zhuoshui River and G3 in the Gaoping River. These two reaches are the transitional sections between hills and plains, which have a 3-fold expansion of valley width compared to the upstream reaches (see Table 2) but still have high energies (the channel slope is 0.072 for Z7 and 0.063 for G3). The active channel width and channel activity also increase with valley width (Figure 7B,C). The joining of large tributaries downstream not only expand the valley width but also increase flow discharge, thus active channel width enlarges too. Moreover, a wider valley increases the freedom for channel migration, which implies that the channel paths are highly changeable in the settings of frequent flood events mainly induced by typhoons.

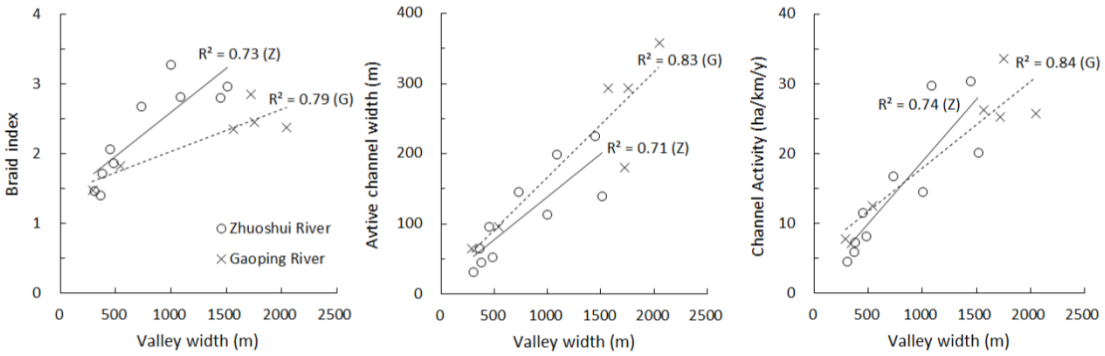


**Figure 7.** The x-y plots for relationships between valley width and braid index (**A**); active channel width (**B**); and channel activity (**C**) in the study reaches.

Although the braid index has an overall positive correlation with valley width, the downstream patterns of braid index show that after reaching a peak value it slightly decreases in the downstream areas in both study rivers (see Figure 4A,D). This should be attributed to the transformation of channel types. In the lowland plains, widening valley width couples with decreasing valley slope and sediment size, making channel planform turn from multiple (braided) channels into a single wandering or straight channel [15–17]. During the process, stream power decreases and channel stability increases. Comparing the lowland reaches between these two rivers, the lowland reaches in the Gaoping River (G4–G6) have a wider valley width as well as a gentler valley slope than the Zhuoshui River (Z8-Z10) (See Table 2). These characteristics result in the braid index in the Gaoping lowland reaches being smaller than in the Zhuoshui River, which results in the slope of the regression line in the Gaoping River being lower than that of the Zhuoshui River (Figure 7A). In fact, observing the channel planform in lowland reaches from the satellite images, mid-channel bars are still distributed along the lower Zhuoshui River in some locations (Figure 8A). By contrast, single or wandering channel(s) are found along the lower Gaoping River (Figure 8B).

Apart from valley width, hydraulic construction could be an artificial factor influencing the downstream changes of channel planform. The downstream patterns of channel planform indices show that evident drop in reach Z6. The upstream end of this reach is the Jiji Weir, a large hydraulic construction (15 m in height) across the river with 18 sluice gates. After being operated since 2001, a large amount of sediment generated from the mountain area was trapped and deposited in the storage space. For the downstream reach, by contrast, the shortage of water and sediment supply restricted reach Z6 from developing multiple channels. This induced significant bedrock erosion (Figure 8C). Bedrock exposure on the channel bed even in wet seasons resulted in a relatively low channel activity. The Gaoping River also has a hydraulic construction named the Gaoping River Weir. Unlike the Jiji Weir, it is a flexible rubber dam and only raises the water level for water intake but no water storage. Besides, it only operates during wet seasons. Therefore, this weir minimizes the impacts on environment and ecology because the longitudinal continuity can be maintained. It does not cause a difference in channel planform indices between its upstream reach (G5) and downstream reach (G6).

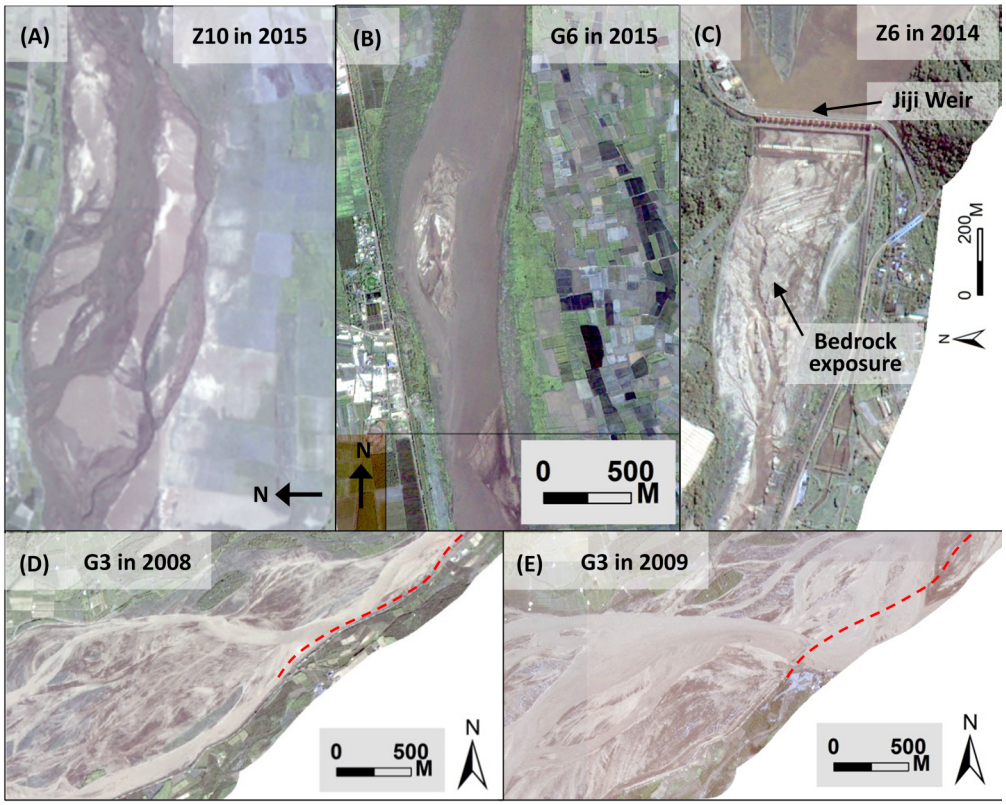


**Figure 8.** Satellite images: (**A**) the braided channels in reach Z10; (**B**) a single/wandering channel in G6; (**C**) bedrock exposure downstream of the Jiji Weir; (**D**) braided channels before Typhoon Morakot in G3; and (**E**) channel expansion and embankment breaking after Typhoon Morakot.

### *5.2. The Influence of Extreme Hydrological Events*

River morphology is formed mainly by hydrological events. The changes of erosion/deposition areas for these two rivers (Figure 5) could link up with the hydrograph (Figure 2) for exploring the channel responses to flood events. During the whole study period, the greatest erosion and deposition areas appeared in the first two periods. Both study rivers show that the greatest erosion occurred in 2008–2009, whereas the greatest deposition occurred in 2009–2010 (Figure 5). Furthermore, the magnitude of the area in the Gaoping River was larger than that of the Zhuoshui River. Obviously, this large variation was caused by Typhoon Morakot in 2009 (Figure 5), which is not only the greatest hydrological event during the study period but also a catastrophic flood with a 200-year return period. Extremely high daily discharges were recorded at Liling Bridge on the Gaoping River (15,251 m3·s$^{-1}$) and Xizhou Bridge on the Zhuoshui River (11,338 m3·s$^{-1}$) on 9 August 2009 (Figure 2). Typhoon Morakot not only reconfigured the distribution of channels and bars but also expanded active channel area, and even breached the embankment in many places along the Gaoping River (Figure 8D,E). In the year 2010, only a few annual flood events occurred, which gradually conveyed massive sediment previously generated in the upstream area to the downstream area, then deposited sediment in river channels, causing a large deposition area to form in the period 2009–2010. Bertoldi et al. [2] analyzed a gravel-bed braided river in Italy and suggested a fundamental difference between two types of flood events of differing magnitude and frequency. Larger floods (with a return period longer than two years) induce a complete reworking of the network configuration rather than a few changes on active branches, as in the case of annual floods (see also [26]). Similar findings were found in our study; events of differing magnitudes play different roles in forming the channel morphology [27].

Although the magnitudes of channel activity during other periods were smaller than the first two periods, the changed areas were always larger than the non-changed areas, especially in the Zhuoshui River (Figure 5). The Zhuoshui and Gaoping Rivers could be of the typical river type in

Taiwan where the tectonic, geological, and hydrological forcing is strong. Taiwan's rivers are characterized by abundant sediment, steep slope with high energy, and high variation in seasonal discharge. As a consequence, channels are sensitive to floods and the channel planform displays a highly dynamic pattern. These characteristics are distinct from other studies in settings with a relative lower frequency of disturbances. For example, the paper by Nelson et al. [13] showed that the largest changes of braid index, active channel width, and channel activity are 1.8, 50 m, and 0.9 ha/km/year respectively. In contrast, our study showed much greater values in Taiwan's rivers, which are 2.5, 200 m, and 50 ha/km/year respectively (see Table 2).

### *5.3. Application of Channel Planform Indices*

Nelson et al. [13] used river indices such as braid index, active channel width, and channel activity to analyze the spatial patterns of channel changes along the Snake River and evaluate the impact of the Jackson Lake Dam. This study adopted these indices, then developed them for usage in three levels. Firstly, a series of values of one index could be analyzed to detect the spatial difference (e.g., downstream pattern from mountain area to lowland) or temporal variation (e.g., annual changes due to flood events) (see Table 2). Secondly, the CV for an index during a period could be used to compare the channel stability between reaches. The value of CV is derived from dividing standard deviation by mean. The analysis in Section 5.2 (Figure 7) shows highly positive correlations between the mean of the three indices and the valley width. Thus, the value of CV could be seen as a reference to the level of variance with normalization by valley width. This is meaningful when comparing reaches between hilly and lowland areas. Overall, the values of indices in lowland reaches are higher than in hilly areas. However, a much wider valley width provides enough space for channel migration. Thus, unstable channels do not necessarily threaten villages along the riversides except in catastrophic events, due to the long distances to the river and the protection of embankments. By contrast, the hilly reaches have lower values of indices but much narrower valley width than the lowland reaches. Moreover, the villages and roads are distributed close to the riversides. As long as channels migrate to the steep side slopes during flood events, strong erosion could occur and thus induce disasters. For example, many villages experienced serious destruction along the Chenyoulan River after Typhoon Toraji in 2001, and along the Laonong River during Typhoon Morakot in 2009. Finally, the values of CV could be added up to obtain a Sensitivity Index as a reference for river authorities when making priorities in river regulation strategy. This study used equal weights for the three indices. The weight could conceivably be adjusted to fit the environmental settings in future studies with the aim of getting a more objective Sensitivity Index. These indices for evaluating channel stability could also be used when comparing rivers in different regions. However, the meaning of the numbers still needs to be put into the context of the river types and their environmental settings.

## 6. Conclusions

This study analyzed braid index, active channel width, and channel activity along two sediment-rich rivers, the Zhuoshui River and the Gaoping River in Taiwan, from 2008 to 2015 based on satellite images of FORMOSAT-2. The results showed that the valley width plays a key role in braided degree, active channel width, and channel activity. These channel planform indices increase as valley width expands whereas the braid index decreases slightly close to the river mouth due to the change of channel types. The downstream patterns were interrupted by large hydrological construction which resulted in limited changes downstream of the weir due to the lack of water and sediment supply. The highly active landscape in Taiwan results in very sensitive channels compared to other regions. A 200-year flood, Typhoon Morakot in 2009, induced significant channel changes in these two rivers. An integrated Sensitivity Index was proposed for identifying unstable reaches, which could be a useful reference for river authorities when making priorities in river regulation strategy. This study shows that satellite image monitoring coupled with river indices analysis could be an effective tool to evaluate spatial and temporal changes in channel stability in highly dynamic river systems.

**Acknowledgments:** The authors are thankful for Jia-En Chen and Jie Li for helping with the satellite image processing and channel digitizing.

**Author Contributions:** Cheng-Wei Kuo carried out image analysis, wrote the manuscript and plotted figures; Chi-Farn Chen collected satellite images and developed the study concept; Su-Chin Chen provided insightful thoughts on channel morphology changes and revised the manuscript; Tun-Chi Yang compensated the influence of hydraulic construction; Chun-Wei Chen analyzed the numerical data.

**Conflicts of Interest:** The authors declare no conflict of interest.

## References

1. Brierley, G.J. Landscape memory: The imprint of the past on contemporary landscape forms and processes. *Area* **2010**, *42*, 76–85.
2. Bertoldi, W.; Zanoni, L.; Tubino, M. Assessment of morphological changes induced by flow and flood pulses in a gravel bed braided river: The Tagliamento river (Italy). *Geomorphology* **2010**, *114*, 348–360.
3. Gilvear, D.J. Fluvial geomorphology and river engineering: Future roles utilizing a fluvial hydrosystems framework. *Geomorphology* **1999**, *31*, 229–245.
4. Ashmore, P.; Parker, G. Confluence scour in coarse braided streams. *Water Resour. Res.* **1983**, *19*, 392–402.
5. Ashmore, P.; Church, M. Sediment transport and river morphology: A paradigm for study. In *Gravel-Bed Rivers in the Environment*; Klingeman, P., Beschta, R., Komar, P., Bradley, J., Eds.; Water Resources Publications LLC: Littleton, CO, USA, 1998; pp. 115–148.
6. Egozi, R.; Ashmore, P. Defining and measuring braiding intensity. *Earth Surf. Processes Landf.* **2008**, *33*, 2121–2138.
7. Zanoni, L.; Gurnell, A.; Drake, N.; Surian, N. Island dynamics in a braided river from analysis of historical maps and air photographs. *River Res. Appl.* **2008**, *24*, 1141–1159.
8. Comiti, F.; Da Canal, M.; Surian, N.; Mao, L.; Picco, L.; Lenzi, M.A. Channel adjustments and vegetation cover dynamics in a large gravel bed river over the last 200 years. *Geomorphology* **2011**, *125*, 147–159.
9. Zinger, J.A.; Rhoads, B.L.; Best, J.L. Extreme sediment pulses generated by bend cutoffs along a large meandering river. *Nat. Geosci.* **2011**, *4*, 675–678.
10. Sarma, J.N. Fluvial process and morphology of the Brahmaputra River in Assam, India. *Geomorphology* **2005**, *70*, 226–256.
11. Takagi, T.; Oguchi, T.; Matsumoto, J.; Grossman, M.J.; Sarker, M.H.; Matin, M.A. Channel braiding and stability of the Brahmaputra river, Bangladesh, since 1967: GIS and remote sensing analyses. *Geomorphology* **2007**, *85*, 294–305.
12. Boruah, S.; Gilvear, D.J.; Hunter, P.; Sharma, N. Quantifying channel planform and physical habitat dynamics on a large braided river using satellite data—The Brahmaputra, India. *River Res. Appl.* **2008**, *24*, 650–660.
13. Nelson, N.C.; Erwin, S.O.; Schmidt, J.C. Spatial and temporal patterns in channel change on the snake river downstream from Jackson lake dam, Wyoming. *Geomorphology* **2013**, *200*, 132–142.
14. Fuller, I.C. Geomorphic impacts of a 100-year flood: Kiwitea stream, Manawatu catchment, New Zealand. *Geomorphology* **2008**, *98*, 84–95.
15. Chen, S.-C.; Shin, P.-Y.; Wu, C.-H. Sediment influence associated with extreme events on the channel pattern in the Chenyoulan River. *J. Chin. Soil Water Conserv.* **2013**, *44*, 311–323.
16. Chen, S.-C.; Shin, P.-Y.; Wu, C.-H.; Chao, Y.-C. The influence of macro-sediment from mountainous areas on the river morphology in the Heshe River. *J. Chin. Soil Water Conserv.* **2013**, *44*, 302–310.
17. Davies, T.R.H.; Korup, O. Persistent alluvial fanhead trenching resulting from large, infrequent sediment inputs. *Earth Surf. Processes Landf.* **2007**, *32*, 725–742.
18. Kao, S.J.; Milliman, J.D. Water and sediment discharge from small mountainous rivers, Taiwan: The roles of lithology, episodic events, and human activities. *J. Geol.* **2008**, *116*, 431–448.
19. Wu, C.H.; Chen, S.C.; Chou, H.T. Geomorphologic characteristics of catastrophic landslides during typhoon Morakot in the Kaoping watershed, Taiwan. *Eng. Geol.* **2011**, *123*, 13–21.
20. Brierley, G.J.; Fryirs, K.A. *Geomorphology and River Management: Applications of the River Styles Framework*; Blackwell: Oxford, UK, 2005.
21. Mosley, M.P. Semi-determinate hydraulic geometry of river channels, South Island, New Zealand. *Earth Surf. Processes Landf.* **1981**, *6*, 127–137.

22. Church, M. Geomorphic response to river flow regulation: Case studies and time- scales. *Regul. Rivers Res. Manag.* **1995**, *11*, 3–22.
23. Boix-Fayos, C.; Barberá, G.G.; López-Bermúdez, F.; Castillo, V.M. Effects of check dams, reforestation and land-use changes on river channel morphology: Case study of the Rogativa catchment (Murcia, Spain). *Geomorphology* **2007**, *91*, 103–123.
24. Phillips, J.D.; Slattery, M.C.; Musselman, Z.A. Channel adjustments of the lower trinity river, texas, downstream of Livingston dam. *Earth Surf. Processes Landf.* **2005**, *30*, 1419–1439.
25. An, H.P.; Chen, S.C.; Chan, H.C.; Hsu, Y. Dimension and frequency of bar formation in a braided river. *Int. J. Sediment Res.* **2013**, *28*, 358–367.
26. Surian, N.; Mao, L.; Giacomin, M.; Ziliani, L. Morphological effects of different channel-forming discharges in a gravel-bed river. *Earth Surf. Processes Landf.* **2009**, *34*, 1093–1107.
27. Kuo, C.W.; Brierley, G.; Chang, Y.H. Monitoring channel responses to flood events of low to moderate magnitudes in a bedrock-dominated river using morphological budgeting by terrestrial laser scanning. *Geomorphology* **2015**, *235*, 1–14.